Circulation: Arrhythmia and Electrophysiology

ORIGINAL ARTICLE

Cardiac Afferent Denervation Abolishes Ganglionated Plexi and Sympathetic Responses to Apnea

Implications for Atrial Fibrillation

Liliana Tavares, MD
Moisés Rodríguez-Mañero, MD, PhD
Bahij Kreidieh, MD
Sergio H. Ibarra-Cortez, MD
Jiexiao Chen, BS
Sufen Wang, PhD
Judit Markovits, DVM, PhD
Roberto Barrios, MD
Miguel Valderrábano, MD

BACKGROUND: The autonomic nervous system response to apnea and its mechanistic connection to atrial fibrillation (AF) are unclear. We hypothesize that sensory neurons within the ganglionated plexi (GP) play a role. We aimed to delineate the autonomic response to apnea and to test the effects of ablation of cardiac sensory neurons with resiniferatoxin (RTX), a neurotoxic TRPV1 (transient receptor potential vanilloid 1) agonist.

METHODS: Sixteen dogs were anesthetized and ventilated. Apnea was induced by stopping ventilation until oxygen saturations decreased to 80%. Nerve recordings from bilateral vagal nerves, left stellate ganglion, and anterior right GP were obtained before and during apnea, before and after RTX injection in the anterior right GP (protocol 1, n=7). Atrial effective refractory period and AF inducibility on single extrastimulation were assessed before and during apnea, and before and after intrapericardial RTX administration (protocol 2, n=9). GPs underwent immunohistochemical staining for TRPV1.

RESULTS: Apnea increased anterior right GP activity, followed by clustered crescendo vagal bursts synchronized with heart rate and blood pressure oscillations. On further oxygen desaturation, a tonic increase in stellate ganglion activity and blood pressure ensued. Apnea-induced effective refractory period shortening from 110.20±31.3 ms to 90.6±29.1 ms (P<0.001), and AF induction in 9/9 dogs versus 0/9 at baseline. After RTX administration, increases in GP and stellate ganglion activity and blood pressure during apnea were abolished, effective refractory period increased to 126.7±26.9 ms (P=0.0001), and AF was not induced. Vagal bursts remained unchanged. GP cells showed cytoplasmic microvacuolization and apoptosis.

CONCLUSIONS: Apnea increases GP activity, followed by vagal bursts and tonic stellate ganglion firing. RTX decreases sympathetic and GP nerve activity, abolishes apnea's electrophysiological response, and AF inducibility. Sensory neurons play a role in apnea-induced AF.

VISUAL OVERVIEW: A visual overview is available for this article.

Key Words: atrial fibrillation ■ autonomic nervous system ■ obstructive sleep apnea ■ sensory neurons ■ TRPV

https://www.ahajournals.org/journal/circep

WHAT IS KNOWN?

- The precise mechanisms for the association between obstructive sleep apnea and atrial fibrillation (AF) are unclear, but a prominent role of the autonomic nervous system is suspected.
- Radiofrequency ablation of the intrinsic cardiac autonomic nervous system (intrinsic cardiac ganglionated plexi [GP]) inhibits apnea-induced AF.

WHAT THE STUDY ADDS?

- Apnea induces a complex response of the autonomic nervous system including intrinsic cardiac GP firing, phasic vagal bursts coinciding with heart rate and blood pressure oscillations, and tonic stellate ganglion firing that lead to atrial effective refractory period shortening and increased AF inducibility.
- Chemical ablation of GP sensory neurons with resiniferatoxin, a neurotoxic TRPV1 (transient receptor potential vanilloid 1) agonist, decreases GP and stellate ganglion activity, abolishes apnea's electrophysiological response, and inhibits AF induction.
- GP sensory neurons play a role in apnea-induced AF and could potentially be therapeutically targeted.

Obstructive sleep apnea (OSA) is associated with atrial fibrillation (AF). The precise mechanisms of apnea-induced susceptibility to AF are unclear. Numerous possible mechanisms responsible for this association have been proposed including autonomic dysfunction.

Apnea induces a response of the cardiac autonomic nervous system (ANS) that may increase AF vulnerability.[1–3] The cardiac ANS comprises the extrinsic cardiac autonomic system, centrally derived parasympathetic and sympathetic nerves, and the intrinsic cardiac autonomic system, which consists of epicardial ganglionated plexi (GP) embedded in fat pads that contain efferent parasympathetic and sympathetic neurons, interneurons, afferent sensory neurons, and others.[4,5] The integrated response of the ANS to apnea and its role in AF susceptibility have not been delineated. Of particular interest is that GP sensory neurons are thought to mediate a local neurosensory reflex in response to mechanical or chemical stimuli, such as acidosis, hypoxia, and hypercarbia, mediated by substance P,[6,7] CGRP (calcitonin gene-related peptide),[6] and others. We hypothesized apnea could be a potent stimulator of sensory neurons.

Resiniferatoxin (RTX; Figure 1A), an ultrapotent analog of capsaicin, the active compound of chili peppers,[8,9] causes the TRPV1 (transient receptor potential vanilloid 1), present in sensory neurons, to become permanently permeable to cations,[10] particularly the calcium cation, leading to a powerful stimulation effect followed by neuronal death, desensitization, and analgesia.[11–13] RTX has been shown to reduce sympathetic activation and cardiac remodeling in heart failure.[14]

We sought to delineate the autonomic response to apnea, its hemodynamic and electrophysiological correlates, and to test the effects of chemical ablation of cardiac GP sensory neurons with RTX.

METHODS

The data that support the findings of this study are available from the corresponding author on reasonable request.

The animal protocol used was approved by the Institutional Animal Care and Use Committee of the Houston Methodist Hospital. A detailed description of the methods is available in the Data Supplement. A total of 16 mongrel dogs were intubated and ventilated (Harvard Apparatus Co, Natick, MA) under general anesthesia. Apnea was induced by disconnecting the ventilator tube at end expiration until oxygen saturation (Sao_2) dropped at least to 80%.

Protocol 1

Under continuous electrocardiographic and hemodynamic monitoring, after median cervical incision and sternotomy, the anesthesia agent was switched to alpha-chloralose. Bilateral vagal, left stellate ganglion (SG), and anterior right GP (ARGP) nerve recordings were obtained (n=7) before and during apnea episodes, before and after local RTX injection in the ARGP (Figure 1B through 1E).

Epicardial fat pads known to contain the anterior right, right and left inferior, and left superior GPs were sampled and the following histological studies were performed: hematoxylin and eosin (H&E) staining and TRPV1 and CGRP immunohistochemical staining. Terminal deoxynucleotidyl transferase dUTP-mediated nick end labeling (TUNEL) assay was also performed to detect apoptotic cells.

Protocol 2

Left atrium geometry maps were performed after a transseptal puncture using NavX guidance. A subxiphoid pericardial puncture was performed and a sheath inserted in the oblique sinus. Effective refractory period (ERP) measurements were measured in 3 sites in the left atrium before and during apnea, before and after intrapericardial RTX injection (Figure 1F through 1I).

Figure 1 shows a schematic representation of both protocols.

RESULTS

Protocol 1

Autonomic Response to Apnea

ARGP Activity

At apnea initiation, sparse bursts of GP activity were noted, which appeared to subside shortly thereafter. As apnea progressed and Sao_2 declined, a consistent increase in GP activity was seen. Figure 2A illustrates GP

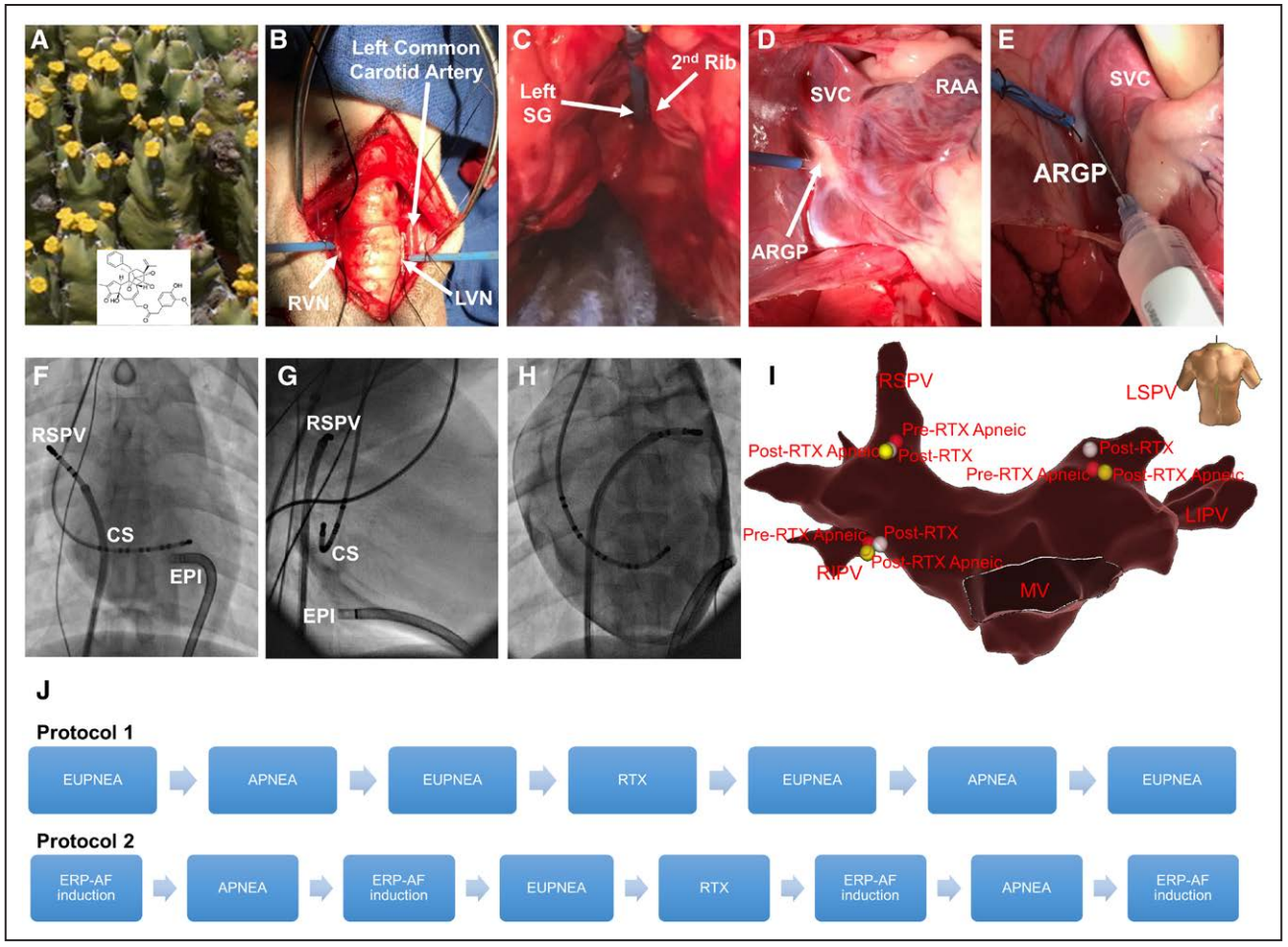

Figure 1. Overview of protocols 1 and 2.
A, Euphorbia resinifera, a cactus-like plant from where resiniferatoxin (RTX) is obtained. Representative examples of cervical right vagal nerve (RVN) and left vagal nerve (LVN; **B**), left stellate ganglion (SG; **C**), and anterior right ganglionated plexi (ARGP; **D**) with recording electrodes. Location of RTX injection in ARGP (**E**). Anteroposterior fluoroscopic view showing the sheath in the epicardium (EPI), the decapolar catheter in the coronary sinus (CS) and the deflectable catheter placed in the right superior pulmonary vein (RSPV; **F**). **G**, Right anterior oblique view. **H**, Left anterior oblique view after epicardial contrast. **I**, Electroanatomical 3-dimensional reconstruction (anteroposterior view) of the left atrium displaying the 3 locations points studied, RSPV (location 1), left superior pulmonary vein (LSPV; location 2), and right inferior pulmonary vein (RIPV; location 3). **J**, Schematic representation of protocols 1 and 2. RAA indicates right atrial appendage; and SVC, superior vena cava.

activity at baseline and during apnea, noted to be most intense at 2 minutes of apnea.

Vagal Activity

Immediately on initiation of apnea, no detectable changes were present in the vagal recordings. However, as Sao_2 declined, crescendo phasic bursts of vagal discharges appeared, which coincided with heart rate (HR) and blood pressure (BP) oscillations. The onset of detectable bursts occurred after 104.97±44.33 seconds into apnea, when Sao_2 was 91.85±6.12%. Each burst coincided with HR and BP changes. Figure 3 shows an example, including vagal activity quantification divided by tertiles. The progressive increase in vagal bursts during apnea was significant (from burst onset to apnea end, all tertiles $P<0.001$, significance level set at $P<0.017$). The number of spikes per burst, the duration and density of bursts (spikes per burst duration) increased, and the interburst delay (time between bursts) decreased significantly in the final tertile towards the end of apnea. Of note, the phasic bursts coincided in all cases with the upsloping phase of HR and the downsloping phase of BP oscillations, whose frequency matched the burst frequency. The phasic relationship between vagal bursts and HR-BP oscillations was consistent in all animals.

Sympathetic Activity

On apnea initiation, a decrease in SG amplitude was seen, but as apnea continued and Sao_2 declined, there was a progressive increase in SG recording amplitude that coincided with HR and BP increases (BP rebound; Figure 4A). The increase in SG activity, contrary to vagal firings, had a tonic pattern rather than phasic bursts. The SG amplitude began to increase as Sao_2 declined to an average of 93.24±5.15%, and persisted beyond resumption of breathing for 65.67±38.84 seconds, closely matching the rebound HR and BP. Subcutaneous nerve activity as an estimate of the sympathetic tone[15] closely matched that of the SG, as recorded in 3

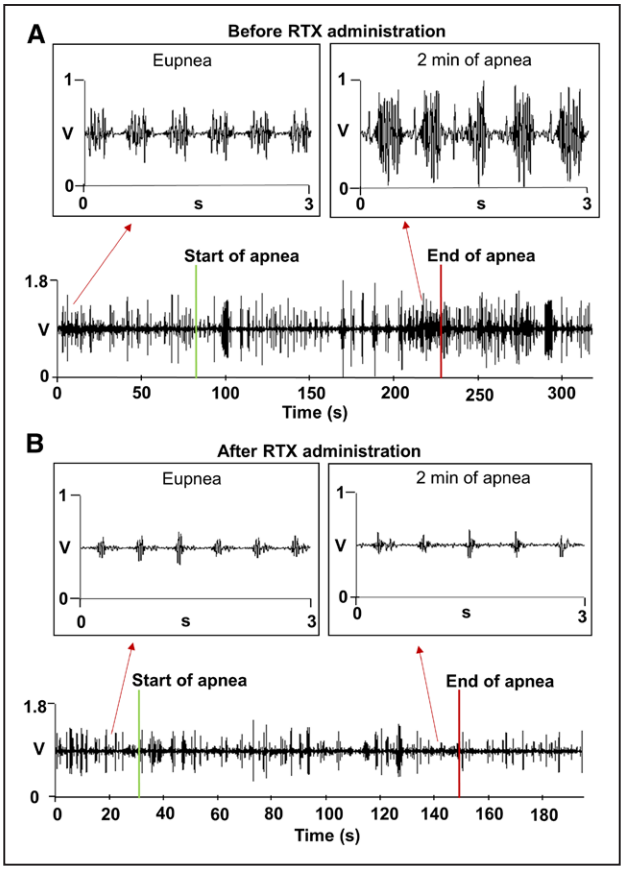

Figure 2. Anterior right ganglionated plexi (ARGP) activity during apnea before and after local resiniferatoxin (RTX) injection.
A, An example of ARGP activity during apnea before RTX injection. On apnea initiation no discernible changes in GP activity were seen, but as apnea progressed and oxygen saturation (Sao_2) declined, GP activity increased, with the highest increase in activity noted at 2 min of apnea with a Sao_2 of 85%. **B**, An example of ARGP activity during apnea after RTX injection. GP recordings after RTX showed no increased activity during apnea.

dogs. Figure 4B shows SG and subcutaneous responses to apnea.

Vagal, SG, and GP nerve activity recovered back to baseline values once apnea was terminated.

Acute GP-RTX–Induced Changes

ARGP RTX injection led to dramatic increases in BP within <20 minutes of infusion in all animals, which more than doubled. HR also increased but less dramatically. Figure 5A illustrates an example of immediate RTX-induced changes caused by local RTX injection. The increases in BP were paralleled by increases in ARGP activity (Figure 5B). Eventually, hemodynamic changes subsided. Time from RTX administration to renormalization of BP and HR ranged from 15 to 40 minutes.

Autonomic Response to Apnea After RTX Administration

Following recovery from acute RTX effects, the baseline hemodynamics in eupneic state were regained. In contrast to baseline recordings, GP and SG recordings during apnea after RTX activity showed no detectable increased activity during apnea (Figures 2B and 4C). Additionally, the BP rebound increase on late desaturation was blunted (Figure 4C; Figures I and II in the Data Supplement).

Vagal nerve activity, however, did not change, with preserved phasic bursts during desaturation and preserved phasic relationship between vagal bursts and HR and BP (Figure III in the Data Supplement). The unaltered vagal response was also shown by the fact that bradycardic responses to cervical vagal stimulation were unaffected by RTX administration (HR decreases of 35±13 bpm versus 34±12 bpm, respectively; P=0.5; Figure IV in the Data Supplement).

Histopathology Studies

All epicardial fat pads sampled contained ganglion cells (Figure 6A) with positive staining for sensory neuronal markers TRPV1 and CGRP. Non-RTX injected GPs (control, saline injected) were positive for TRPV1 and CGRP and cells were not apoptotic (TUNEL-negative; Figure 6A). RTX injected GPs showed individual ganglion cells with cytoplasmic micro and macro vacuolization, had blunted staining for TRPV1 and CGRP, and cells were apoptotic (TUNEL-positive; Figure 6B).

Protocol 2

Electrophysiological Response to Apnea Before RTX Administration

Atrial ERP (AERP) decreased during apnea from 110.20±31.3 ms to 90.6±29.1 ms (P<0.001, significance level set at P<0.025).

AF could only be induced once (4.2%) from a total of 24 eupneic state atrial single extrastimulations. Conversely, during apnea, AF was induced at least once in every single dog. In 24 apneic episodes, AF was successfully induced 14× (58.3%; mean duration=2.23±2.9 minutes), requiring successful cardioversion in 3 episodes (Figure 7).

Electrophysiological Response to Apnea After RTX Administration

Acute hemodynamic and electrocardiographic changes occurred after intrapericardial RTX (Figure 5C and 5D) and fully recovered in 7/9 dogs. These were similar to those observed in protocol 1.

Post-RTX apnea-induced significant increases in AERP from 107.6±23.9 to 126.7±26.9 ms (P<0.001). The eupneic AERP was unchanged from baseline (110.2±31.3 versus 107.6±23.9, P=0.9), which suggests a lack of RTX-induced changes in eupneic myocardial refractoriness.

After RTX, AF could only be induced once (4.2%) from a total of 21 eupneic state atrial single extrastimulations and could no longer be induced during apnea in any of the 21 apneic induction attempts performed.

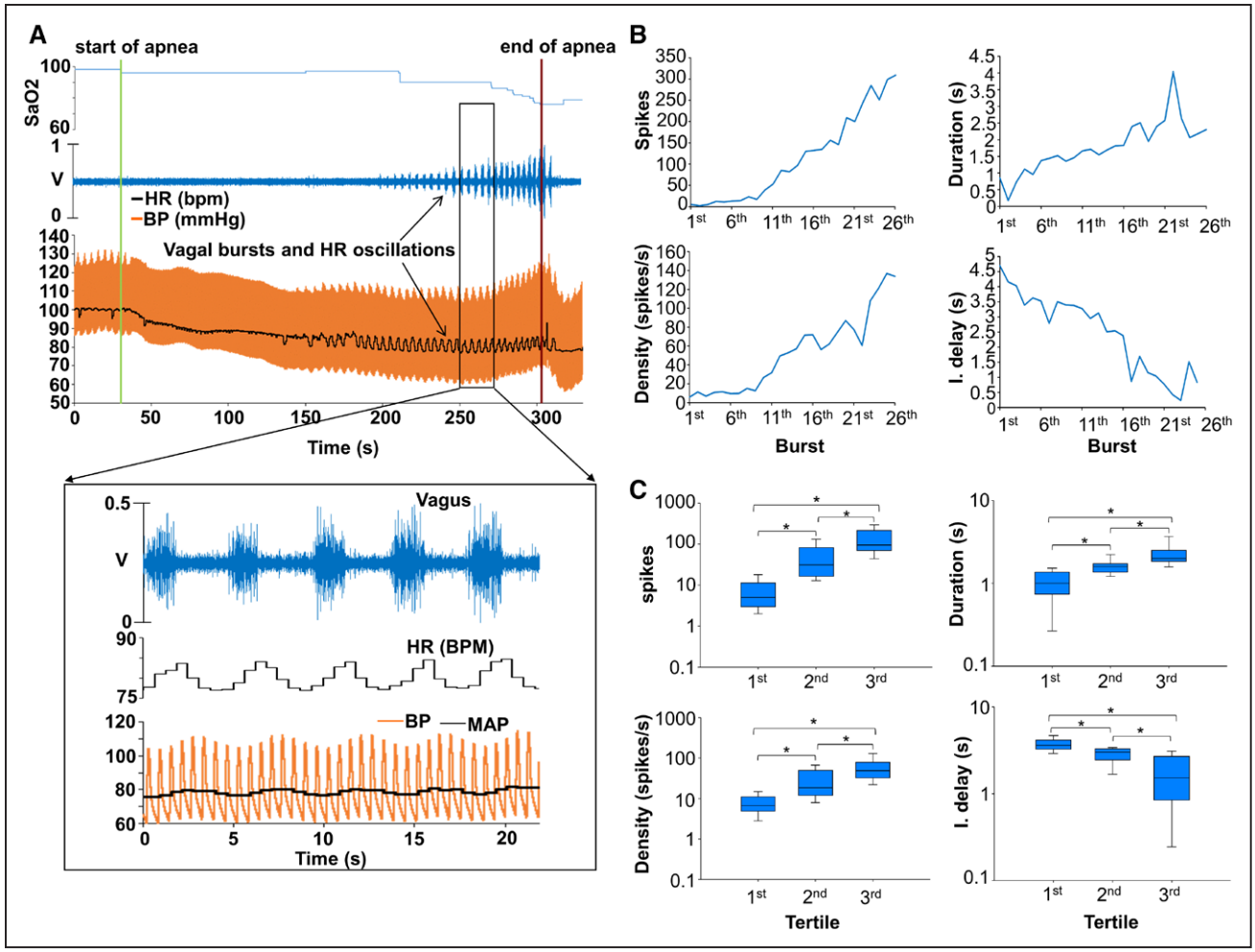

Figure 3. Vagal activity during apnea before resiniferatoxin (RTX) injection.
A and **B**, Example of vagal nerve activity during apnea before RTX. Initially, no detectable changes were seen in the vagal activity. However, as oxygen saturation (Sao_2) declined changes in the activity occurred, in the form of crescendo phasic bursts of discharges that coincided with heart rate (HR) and blood pressure (BP) oscillations. Vagal bursts started after 2 min and 34 seconds of apnea and with a Sao_2 of 97%. The number of spikes, the duration, and the density (spikes/duration) of each burst progressively increased as apnea continued. The time interval between bursts (interburst delay) decreased. **C**, Vagal burst activity during apnea divided in tertiles. A progressive and significant increase in vagal bursts during apnea was observed (from burst onset to apnea end, all tertiles $P<0.001$). Data expressed as median and interquartile range. *Statistical significance set at $P<0.017$. MAP indicates mean arterial pressure.

DISCUSSION

Our studies show several novel findings. First, we delineate the integrated autonomic response to apnea, which includes a consistent sequence of events on oxygen desaturation (Graphic Abstract), including: (1) increases in GP activity; (2) progressively increasing phasic bursts of vagal activity, which closely correlate with HR and BP oscillations; and (3) tonic increase in sympathetic activity, which correlates with steady increases in HR and systolic BP. Second, we correlate these autonomic changes with electrophysiological changes, namely ERP shortening and consistent AF induction with single extrastimulation during apnea. Third, we show the acute effects of RTX administration, both locally as well as intrapericardially, which are characterized by a dramatic increase in ARGP activity and BP, and increases in HR. Such sympathetic afferent activation, along with its associated hemodynamic effects, can lead to additional electrophysiological changes, including spontaneous ventricular fibrillation but is characteristically transient, and followed by recovery to a baseline physiological state. Fourth, we show that apnea post-RTX lacked ARGP activation, and lacked the increased SG and rebound BP associated with deoxygenation. Additionally, RTX eliminated both apnea-induced AERP shortening and AF inducibility; and after RTX treatment, apnea led to prolonged AERP.

These results are consistent with a fundamental role of the cardiac ANS mediating the electrophysiological responses of the atrial myocardium to apnea and suggest the cardiac afferents as a possible therapeutic target for autonomic modulation.

ANS Response to Apnea: Hemodynamic and Electrophysiological Correlates

The consistent sequence of events we detected seems to initiate with slow, steady decreases in HR followed

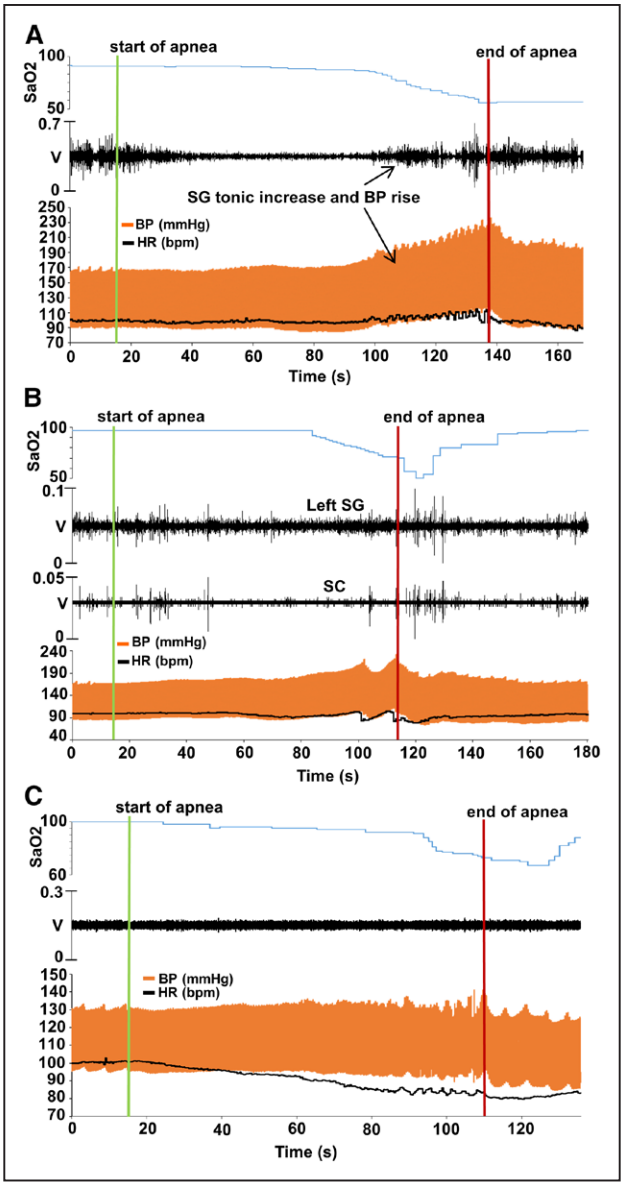

Figure 4. Sympathetic activity during apnea before and after local resiniferatoxin (RTX) injection.
A, An example of stellate ganglion (SG) activity during apnea before RTX injection. Initially, a decrease in SG amplitude was seen, but as apnea continued and oxygen saturation (Sao_2) declined, there was a progressive increase in SG recording amplitude that coincided with heart rate (HR) and blood pressure (BP) increases. SG activity began to increase after 1 min and 21 seconds of apnea and with a Sao_2 of 93%. **B**, SG and subcutaneous (SC) activity during apnea. We observed that SC nerve activity closely matched that of the SG. **C**, An example of SG activity during apnea after RTX injection. The increased SG activity, previously observed, which had correlated with the HR and BP increase was abolished after RTX.

by HR and BP oscillations and later by a BP rebound increase (Graphic Abstract). An initial increase in GP activity subsided to then increase, particularly at the end of apnea. The onset of HR oscillations preceded the onset of phasic bursts of vagal discharges, whose frequency, amplitude, and spike density grew as apnea persisted. The crescendo nature of these bursts was paralleled by an increase in the frequency of HR and BP oscillations, which supports a mechanistic connection. Of note, vagal bursts coincided with the upsloping phase of HR oscillations and the downsloping phase of BP oscillations. The mechanistic origin of such vagal bursts is unclear, but could represent afferent activity since most fibers in the vagal nerves are afferent,[16,17] or originate from sympathetic efferents of the vagus leading to HR increases,[18] or be parasympathetic efferents with either primary effects on BP or delayed effects on HR.

Coinciding with the onset of oxygen desaturation, a tonic increase in sympathetic (SG) activity was found, which matched the onset of a steady increase in BP. Subcutaneous nerve activity matched the SG activity, as previously reported.[15] The GP and SG activity and the BP rebound were abolished by RTX injection.

Role of the ANS and Sensory Neurons in the Genesis of AF in Apnea

Previous experimental studies have demonstrated a close mechanistic association between the cardiac ANS and apnea-induced AF, focusing mainly on parasympathetic contributors.[2,19] In a canine model of apnea, Ghias et al[1] documented increases in neural activity within the GP before the initiation of AF. Furthermore, ablation of the aorta superior vena cava ganglionated plexus significantly diminished the inducibility of AF. We expand their findings to show the orchestrated intrinsic (GP) versus extrinsic ANS (vagal and SG) response to apnea and their changes after RTX.

Sensory neurons are an integral part of the GP. GP local sensory neurons are thought to mediate a local neurosensory reflex within the GP.[20] The overall physiological effect of sensory neurons activation is a depolarization of postganglionic parasympathetic neurons,[21,22] thus enhancing GP output and leading to the local release of acetylcholine and the electrophysiological effects that follow (namely ERP shortening). This effect could be occurring at a local GP level. The mechanical and chemical stimuli to which sensory neurons react under physiological conditions is unclear, but it makes physiological sense to hypothesize that apnea-induced hypoxia, hypercarbia, acidosis, or mechanical stretch may play a role. Our data support such contention.

We propose a reflex model of apnea-induced AF susceptibility. Apnea directly causes hypoxia, hypercarbia, and acidosis. Either by chemoreceptors sensing pH, po_2 or pco_2, or mechanoreceptors sensing increased pressure, sensory neurons would be activated via TRPV1. Sensory neurons have the somata in the dorsal root ganglia, in the nodose ganglion of the vagus, and in the intrinsic cardiac nervous system themselves.[20] Local intrinsic cardiac nervous system sensory neuron activation could activate postganglionic parasympathetic neurons,[21,22] thus form-

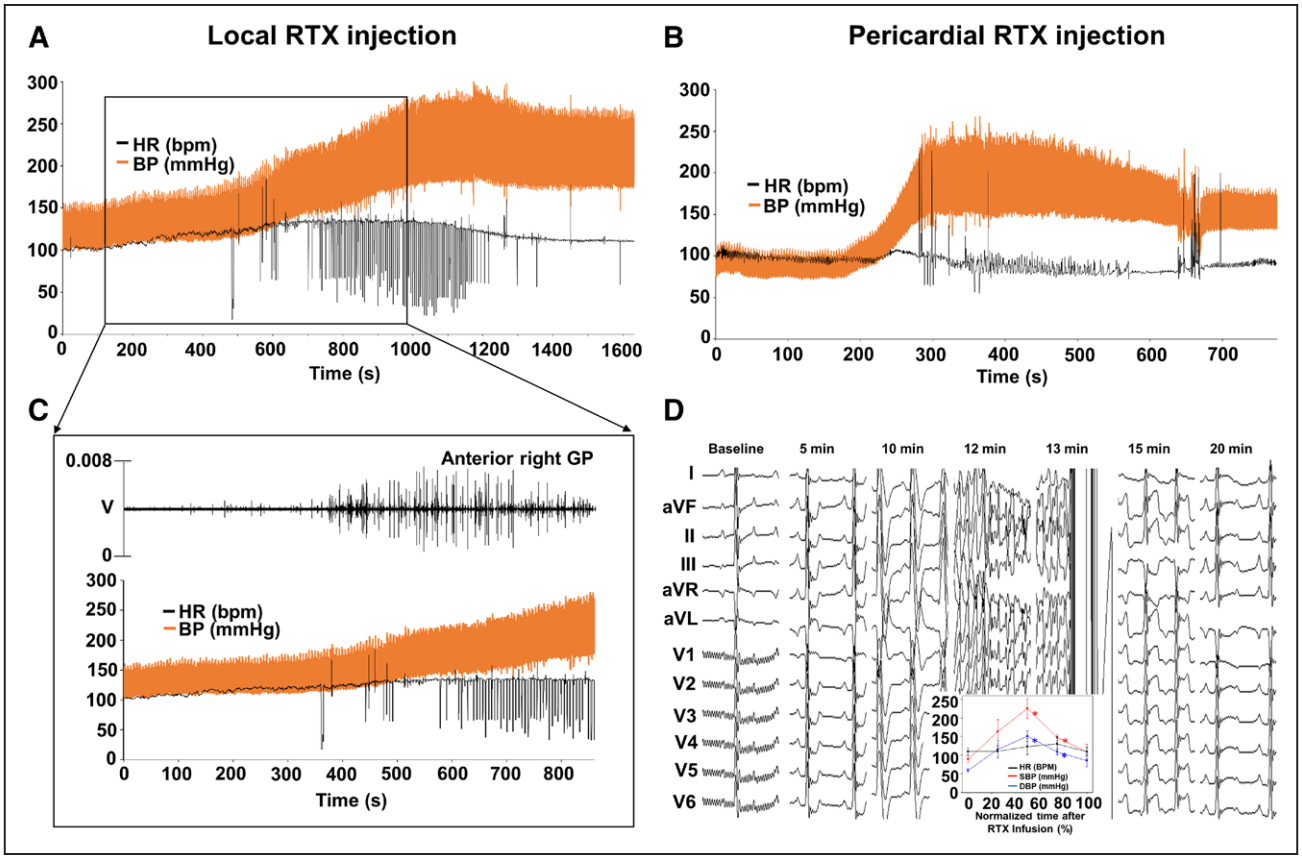

Figure 5. Acute ganglionated plexi (GP)-resiniferatoxin (RTX)–induced changes.
Both routes of injection led to vascular lability with dramatic increases in systolic blood pressure (SBP) within <20 min of infusion in all animals. **A**, An example of immediate RTX-induced changes caused by local RTX injection. Heart rate (HR), SBP, and diastolic blood pressure (DBP) increased within 3 min and 20 seconds of injection. **B**, An example of immediate RTX-induced changes caused by intrapericardial RTX injection. HR, SBP, and DBP increased within 3 min of injection. **C**, Increases in BP and HR were paralleled by increases in anterior right GP activity. **D**, Sequential electrocardiographic changes recorded. ST-segment changes and QRS widening.

ing a local reflex arc that leads to ERP shortening in neighboring myocardium. Sympathetic afferents enter through the stellate ganglia and the spinal cord and terminate in the nucleus of the solitary tract,[23] leading to increased sympathetic outflow. Both the local effect leading to ERP shortening and AF inducibility, as well as the increased sympathetic outflow, are abolished by RTX-induced sensory neuron ablation. Vagal responses were unchanged. The lack of vagal effects suggests that either parasympathetic afferents were not affected, or perhaps more likely, that they are mediated by non-GP afferents, either pulmonary or carotid.

After RTX, apnea-induced prolongation of the ERP rather than shortening. This is consistent with direct myocardial effects of hypoxia, hypercarbia or acidosis, increasing postrepolarization refractoriness, analogous to the myocardial effects of ischemia,[24] which are normally counteracted by the neuronal reflexes described.

Acute RTX Effects

Sensory afferents mediate the cardiac sympathetic afferent reflex, thought to lead to sympathoexcitation in heart failure and acute ischemia.[13] RTX applied to the epicardium in rats can abolish this response,[13,14] and leads to loss of TRPV1-expressing neurons, which in turn has been associated with reduced fibrosis in ischemia-induced heart failure.[14] The acute hemodynamic effects of RTX in vivo have been described.[25] Consistent with transient hyperactivation of cardiac sympathetic afferents, RTX led to marked GP activity, doubling of the systolic BP, increases in HR, and significant electrocardiographic changes (ST elevation, T-wave inversion, and even ventricular fibrillation). These changes completely subsided and normalized over the course of up to 40 minutes, consistent with the time course from RTX-induced activation followed by neuronal toxicity.

Clinical Implications

Sleep apnea is associated with AF. Multiple mechanisms are involved, but a prominent role of the ANS is suspected. Here, we delineate the integrated autonomic response to apnea, that includes GP, vagal, and SG firings in a consistent manner that leads to hemodynamic and electrophysiological (shortened ERP) changes that

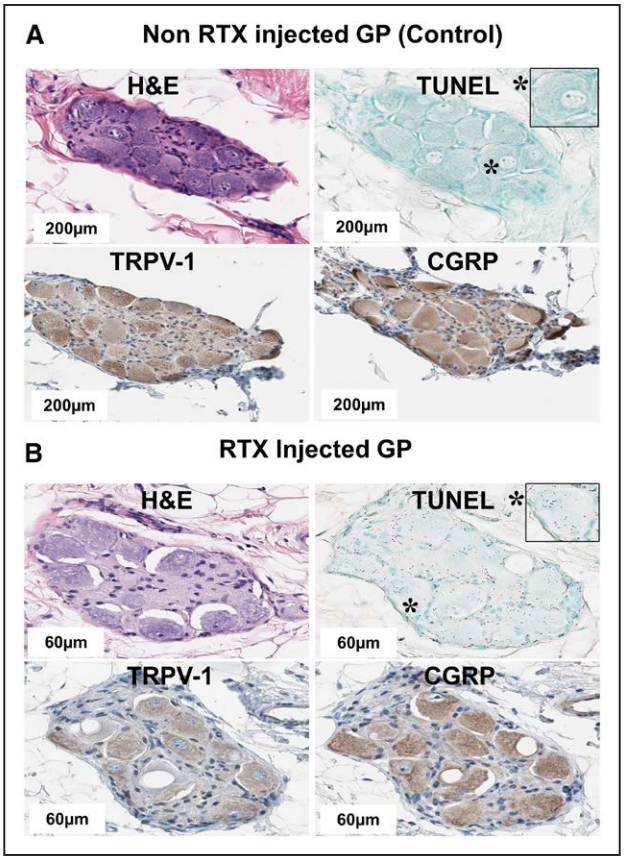

Figure 6. Histopathology studies of the ganglionated plexi (GP). **A**, Hematoxylin and eosin (H&E), terminal deoxynucleotidyl transferase dUTP-mediated nick end labeling (TUNEL), TRPV1 (transient receptor potential vanilloid 1), and CGRP (calcitonin gene-related peptide) staining of non-resiniferatoxin (RTX)–injected GP (control). Individual cells within the ganglion were positive for sensory neuronal markers TRPV1 and CGRP and were not apoptotic (TUNEL-negative). **B**, H&E, TUNEL, TRPV1, and CGRP staining of RTX injected GP. Some individual ganglion cells morphologically displayed cytoplasmic micro and macro vacuolization. Cells bluntly stained for TRPV1 and CGRP and were apoptotic (TUNEL-positive).

culminate in AF inducibility. The GP and SG responses were abolished by sensory neuron ablation with RTX. Sensory neurons mediate the electrophysiological response to apnea and could be a valid therapeutic target to reduce apnea-induced AF.

Study Limitations

OSA-induced AF is multifactorial and is likely to involve a plethora of mechanisms that were not studied here as hypertension, obesity, metabolic syndrome, atrial structural remodeling, among others.[26] The animal model used in this study is merely an acute model, and not an exact replica of OSA as it does not reproduce all events associated with long-term OSA. However, this approach reproduces the hypoxia, hypercarbia, and acidosis of OSA as putative triggers of an autonomic response in an acute model of apnea and eliminates other confounding factors such as obesity, metabolic syndrome, and intrathoracic pressure dynamics that can confound a mechanistic response of the sensory neurons.

Future studies are needed to investigate the chronic effects of chemical ablation of cardiac GP sensory neurons. Chronically repeated OSA episodes has been shown to cause cardiac remodeling with fibrosis playing a prominent role which contributes to AF promotion.[27]

We did not record signals from all GPs as we were limited by anatomic access to the ARGP. Additionally, peripheral blood CO_2 and pH were not monitored. Although the mechanistic implications are significant, basic electrophysiological properties, such as action potential duration, and conduction velocity, were beyond the scope of this study. There could be concerns about the specificity of RTX effects. However, it should be highlighted that prior studies have consistently shown the absence of myocardial effects.[8,10,13]

Conclusions

Apnea leads to a complex response of the cardiac ANS including GP firing, phasic vagal bursts coinciding with HR and BP oscillations, and tonic SG firing that lead to ERP shortening and increased in AF vulnerability. Chemical ablation of intrinsic cardiac sensory neurons with RTX decreases sympathetic and GP nerve activity, and abolishes the electrophysiological response seen during apnea.

A critical role of a neurosensory reflex in apnea-induced AF is suggested and could potentially be therapeutically targeted.

ARTICLE INFORMATION

Received September 29, 2018; accepted April 12, 2019.

The Data Supplement is available at https://www.ahajournals.org/doi/suppl/10.1161/CIRCEP.118.006942.

Correspondence

Miguel Valderrábano, MD, Division of Cardiac Electrophysiology, Department of Cardiology, Houston Methodist Hospital, 6550 Fannin St, Suite 1901, Houston, TX 77030. Email mvalderrabano@houstonmethodist.org

Affiliations

Division of Cardiac Electrophysiology, Department of Cardiology, Houston Methodist DeBakey Heart & Vascular Center, Houston Methodist Hospital (L.T., B.K., S.H.I.-C., J.C., S.W., M.V.), Department of Pathology, Comparative Medicine Program (J.M.), and Department of Pathology, Houston Methodist Hospital (R.B.), Houston Methodist Research Institute, TX. Cardiology Department, Hospital Universitario Santiago de Compostela, Spain (M.R.-M.). Cardiology Department, Hospital Universitario Santiago de Compostela, Instituto de Investigación Sanitaria de Santiago de Compostela (IDIS), Santiago de Compostela, Spain (M.R.-M.). Centro de Investigación Biomédica en Red de Enfermedades Cardiovasculares (CIBERCV CB16/11/00226-CB16/11/00420), Madrid, Spain (M.R.-M.).

Acknowledgments

We thank Holly Zapalac, Daryl Schulz, Caroline White, Courtney Vallien, and Maga Sanchez for their technical assistance.

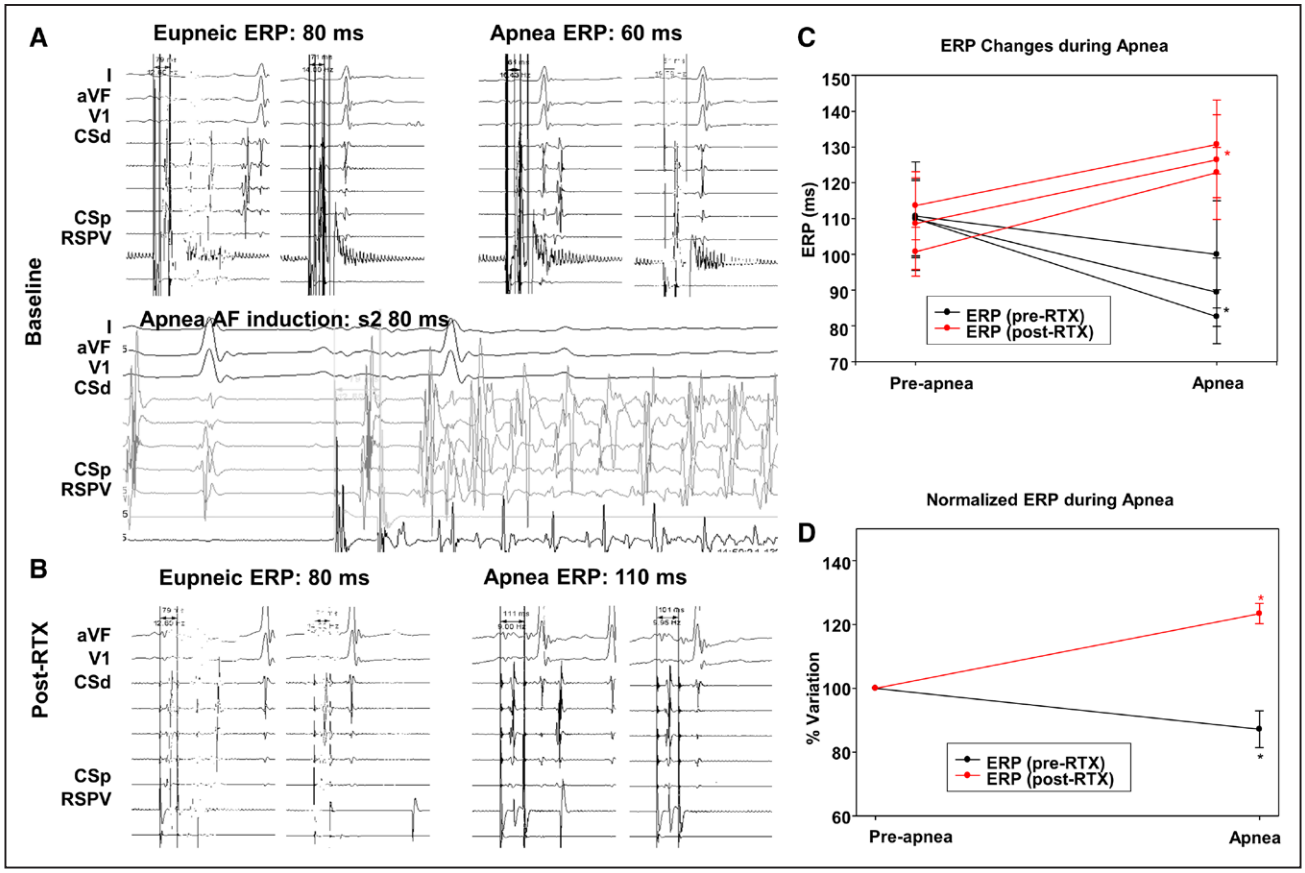

Figure 7. Electrophysiological response to apnea before and after resiniferatoxin (RTX) injection.
A, An example of effective refractory period (ERP) changes during apnea before RTX injection. Apnea led to ERP decrease, from a baseline of 400/80 ms to 400/60 ms, and atrial fibrillation (AF) induction with left atrial single extrastimulation. **B**, An example of ERP changes during apnea after RTX injection. The ERP increased during apnea after RTX injection, from a baseline of 400/80 ms to 400/110 ms. **C**, Absolute atrial ERP changes noted in location 1 (right superior pulmonary vein [RSPV]), location 2 (left superior pulmonary vein [LSPV]), and location 3 (right inferior pulmonary vein [RIPV]) during apneic episodes before (black line) and after (red line) RTX. **D**, Normalized averaged atrial ERP variation during apneic episodes before (black line) and after (red line) RTX. Data expressed as mean±SD. **P*<0.05, significance level set at *P*<0.025. CSd indicates coronary sinus distal; and CSp, coronary sinus proximal.

Sources of Funding

This study was supported by National Institutes of Health/National Heart, Lung, and Blood Institute R01 HL115003 (United States) and the Charles Burnett III and the Lois and Carl Davis Centennial Chair endowments (Houston, TX).

Disclosures

None.

REFERENCES

1. Ghias M, Scherlag BJ, Lu Z, Niu G, Moers A, Jackman WM, Lazzara R, Po SS. The role of ganglionated plexi in apnea-related atrial fibrillation. *J Am Coll Cardiol*. 2009;54:2075–2083. doi: 10.1016/j.jacc.2009.09.014
2. Gao M, Zhang L, Scherlag BJ, Huang B, Stavrakis S, Hou YM, Hou Y, Po SS. Low-level vagosympathetic trunk stimulation inhibits atrial fibrillation in a rabbit model of obstructive sleep apnea. *Heart Rhythm*. 2015;12:818–824. doi: 10.1016/j.hrthm.2014.12.024
3. Linz D, Schotten U, Neuberger HR, Böhm M, Wirth K. Negative tracheal pressure during obstructive respiratory events promotes atrial fibrillation by vagal activation. *Heart Rhythm*. 2011;8:1436–1443. doi: 10.1016/j.hrthm.2011.03.053
4. Ardell J. Structure and function of mammalian intrinsic cardiac neurons. In: Armour JAA, JL, ed. *Neurocardiology*. New York: Oxford University Press; 1994:95–114.
5. Wake E, Brack K. Characterization of the intrinsic cardiac nervous system. *Auton Neurosci*. 2016;199:3–16. doi: 10.1016/j.autneu.2016.08.006
6. Urban L, Papka RE. Origin of small primary afferent substance P-immunoreactive nerve fibers in the guinea-pig heart. *J Auton Nerv Syst*. 1985;12:321–331.
7. Dalsgaard CJ, Franco-Cereceda A, Saria A, Lundberg JM, Theodorsson-Norheim E, Hökfelt T. Distribution and origin of substance P- and neuropeptide Y-immunoreactive nerves in the guinea-pig heart. *Cell Tissue Res*. 1986;243:477–485.
8. Szallasi A, Blumberg PM. Resiniferatoxin, a phorbol-related diterpene, acts as an ultrapotent analog of capsaicin, the irritant constituent in red pepper. *Neuroscience*. 1989;30:515–520.
9. Walpole CS, Bevan S, Bloomfield G, Breckenridge R, James IF, Ritchie T, Szallasi A, Winter J, Wrigglesworth R. Similarities and differences in the structure-activity relationships of capsaicin and resiniferatoxin analogues. *J Med Chem*. 1996;39:2939–2952. doi: 10.1021/jm960139d
10. Caterina MJ, Schumacher MA, Tominaga M, Rosen TA, Levine JD, Julius D. The capsaicin receptor: a heat-activated ion channel in the pain pathway. *Nature*. 1997;389:816–824. doi: 10.1038/39807
11. Szallasi A, Blumberg PM. Vanilloid receptor loss in rat sensory ganglia associated with long term desensitization to resiniferatoxin. *Neurosci Lett*. 1992;140:51–54.
12. Olah Z, Szabo T, Karai L, Hough C, Fields RD, Caudle RM, Blumberg PM, Iadarola MJ. Ligand-induced dynamic membrane changes and cell deletion conferred by vanilloid receptor 1. *J Biol Chem*. 2001;276:11021–11030. doi: 10.1074/jbc.M008392200
13. Zahner MR, Li DP, Chen SR, Pan HL. Cardiac vanilloid receptor 1-expressing afferent nerves and their role in the cardiogenic sympathetic reflex in rats. *J Physiol*. 2003;551(pt 2):515–523. doi: 10.1113/jphysiol.2003.048207
14. Wang HJ, Wang W, Cornish KG, Rozanski GJ, Zucker IH. Cardiac sympathetic afferent denervation attenuates cardiac remodel-

ing and improves cardiovascular dysfunction in rats with heart failure. *Hypertension*. 2014;64:745–755. doi: 10.1161/HYPERTENSIONAHA.114.03699
15. Robinson EA, Rhee KS, Doytchinova A, Kumar M, Shelton R, Jiang Z, Kamp NJ, Adams D, Wagner D, Shen C, Chen LS, Everett TH, Fishbein MC, Lin SF, Chen PS. Estimating sympathetic tone by recording subcutaneous nerve activity in ambulatory dogs. *J Cardiovasc Electrophysiol*. 2015;26:70–78. doi: 10.1111/jce.12508
16. Foley JO, DuBois FS. Quantitative studies of the vagus nerve in the cat. I. The ratio of sensory to motor fibers. *J Comp Neurol*. 1937;67:49–67.
17. Chang RB, Strochlic DE, Williams EK, Umans BD, Liberles SD. Vagal sensory neuron subtypes that differentially control breathing. *Cell*. 2015;161:622–633. doi: 10.1016/j.cell.2015.03.022
18. Onkka P, Maskoun W, Rhee KS, Hellyer J, Patel J, Tan J, Chen LS, Vinters HV, Fishbein MC, Chen PS. Sympathetic nerve fibers and ganglia in canine cervical vagus nerves: localization and quantitation. *Heart Rhythm*. 2013;10:585–591. doi: 10.1016/j.hrthm.2012.12.015
19. Wickramasinghe SR, Patel VV. Local innervation and atrial fibrillation. *Circulation*. 2013;128:1566–1575. doi: 10.1161/CIRCULATIONAHA.113.001596
20. Adams DJC, J. Electrophysiological properties of intrinsic cardiac neurons. In: J. A. A. Armour, J.L., ed. *Basic and Clinical Neurocardiology*. New York: Oxford University Press; 2004:1–60.
21. Konishi S, Otsuka M. Blockade of slow excitatory post-synaptic potential by substance P antagonists in guinea-pig sympathetic ganglia. *J Physiol*. 1985;361:115–130.
22. Hardwick JC, Mawe GM, Parsons RL. Evidence for afferent fiber innervation of parasympathetic neurons of the guinea-pig cardiac ganglion. *J Auton Nerv Syst*. 1995;53:166–174.
23. Cervero F. Sensory innervation of the viscera: peripheral basis of visceral pain. *Physiol Rev*. 1994;74:95–138. doi: 10.1152/physrev.1994.74.1.95
24. Downar E, Janse MJ, Durrer D. The effect of acute coronary artery occlusion on subepicardial transmembrane potentials in the intact porcine heart. *Circulation*. 1977;56:217–224.
25. Yoshie K, Rajendran PS, Massoud L, Kwon O, Tadimeti V, Salavatian S, Ardell JL, Shivkumar K, Ajijola OA. Cardiac vanilloid receptor-1 afferent depletion enhances stellate ganglion neuronal activity and efferent sympathetic response to cardiac stress. *Am J Physiol Heart Circ Physiol*. 2018;314:H954–H966. doi: 10.1152/ajpheart.00593.2017
26. May AM, Van Wagoner DR, Mehra R. OSA and cardiac arrhythmogenesis: mechanistic insights. *Chest*. 2017;151:225–241. doi: 10.1016/j.chest.2016.09.014
27. Iwasaki YK, Kato T, Xiong F, Shi YF, Naud P, Maguy A, Mizuno K, Tardif JC, Comtois P, Nattel S. Atrial fibrillation promotion with long-term repetitive obstructive sleep apnea in a rat model. *J Am Coll Cardiol*. 2014;64:2013–2023. doi: 10.1016/j.jacc.2014.05.077